SYNTHESIS OF PLANAR ARRAYS USING A MODIFIED PARTICLE SWARM OPTIMIZATION ALGORITHM BY INTRODUCING A SELECTION OPERATOR AND ELITISM

M. Lanza, J. R. Pérez, and J. Basterrechea

Department of Communications Engineering
University of Cantabria
Edificio I + D de Telecomunicaciones, Plaza de la Ciencia
Avda, de Los Castros s/n, Santander 39005, Spain

Abstract—A modified particle swarm optimization (PSO) algorithm applied to planar array synthesis considering complex weights and directive element patterns is presented in this paper. The modern heuristic classical PSO scheme with asynchronous updates of the swarm and a global topology has been modified by introducing tournament selection, one of the most effective selection strategies performing in genetic algorithms the equivalent role to natural selection, and elitism. The modified PSO proposed combines the abilities of the classical PSO to explore the search space and the pressure exerted by the selection operator to speed up convergence. Regarding the optimization problem, the synthesis of the feeds for rectangular planar arrays consisting of microstrip patches or subarrays of microstrip patches is considered. Results comparing the performance and limitations of classical and modified PSO-based schemes are included considering both test functions and planar array complex synthesis to best meet certain far-field radiation pattern restrictions given in terms of 3D-masks. Finally, representative synthesis results for sector antennas for worldwide interoperability for microwave access (WiMAX) applications are also included and discussed.

1. INTRODUCTION

The PSO algorithm, based on the movement and intelligence of swarms, has become an attractive alternative to other heuristic

Corresponding author: J. R. Pérez (perezjr@unican.es).

approaches such as genetic algorithms (GA), simulated annealing (SA) or ant colony optimization (ACO), and has been successfully applied in different research areas [1–9]. This work focuses on the analysis of a modified PSO-based approach proposed by the authors to improve the performance of classical schemes.

One of the main advantages of PSO over other stochastic optimization methods such as GA or SA, lies in the ease with which it can be tuned and implemented, using only a velocity operator to drive the search throughout the hyperspace [1]. New modified PSO-based schemes are continuously emerging in the literature in an attempt to improve the overall performance of classical schemes in one direction: to speed up convergence preserving diversity and increasing exploration abilities. Different modified versions of the classical PSO algorithm can be found applied to array synthesis [10, 11], patch antenna design [12] or planar multilayered absorbers design [13]. In fact, there are some schemes that mix up heuristic GA and PSO optimization algorithms [14, 15].

In this work, the PSO approach proposed benefits from some characteristics of GA, introducing a selection operator to direct and speed up the search, the tournament selection strategy, along with elitism, applied to ensure that the best particle within the swarm is preserved iteratively [2]. The approach proposed does not modify the core of the PSO at all, but simply introduces two mechanisms that iteratively imitate natural selection, rewarding the best potential solutions and increasing the search pressure over the apparently most promising areas, although this fact leads to a loss in diversity, which might drive the algorithm to deceptive solutions. The modified PSO proposed has been tested using standard test functions and the improvements achieved when compared to classical PSO demonstrate the usefulness of the hybrid algorithm.

Regarding array synthesis, there are in the literature several PSO related papers. For instance, phase-only, amplitude-only and complex synthesis of linear arrays is accomplished by GA and PSO in [16]. In [17], several PSO algorithms have been applied to the design of non-uniform and thinned arrays. Several modified PSO algorithms can also be found applied to the pattern synthesis of circular arrays or phased arrays [10, 11]. Furthermore, classical and hybrid PSO schemes, [18] and [19] respectively, have also been applied by the authors to linear array synthesis.

This paper is organized as follows. In Section 2, a theoretical description of the planar array synthesis problem is included. The main features of the classical PSO algorithm, as well as the modified approach proposed, are presented in Section 3. Section 4 includes

a wide range of results, comparing in Section 4.1 the performance of both classical and modified PSO schemes using either well-known test functions or a canonical planar array synthesis problem; and summarizing in Section 4.2 representative far-field radiation pattern synthesis results for sector antennas for WiMAX applications. Finally, some conclusions are outlined in Section 5.

2. SYNTHESIS OF PLANAR ARRAYS

The far-field radiation pattern of a planar array at an arbitrary direction (θ, ϕ) when mutual coupling effects between elements are neglected, is given by

$$FF(\theta, \phi) = EP(\theta, \phi) \cdot AF(\theta, \phi) \tag{1}$$

in which $EP(\theta, \phi)$ represents the element pattern and $AF(\theta, \phi)$ is the array factor.

Let us consider a planar array consisting of $M \times N$ elements lying on the xy plane, parallel to the axes and uniformly spaced a distance d_x and d_y on the x and y axes, respectively. Then, the array factor is given by

$$AF(\theta, \phi) = \sum_{m=0}^{M-1} \sum_{n=0}^{N-1} a_{mn} \cdot e^{j(m \cdot k_x \cdot d_x + n \cdot k_y \cdot d_y + \alpha_{mn})} \tag{2}$$

in which a_{mn} and α_{mn} represent the amplitude and phase of the excitation currents for each element within the array, and k_x and k_y are the x and y components of the wavenumber vector.

Regarding the $EP(\theta, \phi)$, rectangular microstrip patches have been considered. The radiated far-fields of this structure are given by expressions (3) and (4), calculated considering the simplified equivalent magnetic currents model [20], that resonance occurs in the y direction, as well as a negligible thickness, h.

$$E_\theta = j \cdot A \cdot \sin(\phi) \cdot \text{sinc}\left(\frac{k_x \cdot a}{2 \cdot \pi}\right) \cdot \cos\left(\frac{k_y \cdot b}{2}\right) \tag{3}$$

$$E_\phi = j \cdot A \cdot \cos(\theta) \cdot \cos(\phi) \cdot \text{sinc}\left(\frac{k_x \cdot a}{2 \cdot \pi}\right) \cdot \cos\left(\frac{k_y \cdot b}{2}\right) \tag{4}$$

In (3)–(4), a, b and h represent the length, width and dielectric thickness, of the microstrip patches; and A is given by (5), in which E_0 is an amplitude constant.

$$A = \frac{E_0 \cdot a \cdot h \cdot 4 \cdot e^{-j \cdot k \cdot r}}{\lambda \cdot r} \tag{5}$$

The radiated co-polar and cross-polar far-field components of each element are calculated according to the first definition of Ludwig [21], considering that planar arrays in this work will be designed to provide horizontal polarization along the y-axis. Consequently, considering complex synthesis (neither progressive phase nor separable excitations), the aim is to optimize the couples (a_{mn}, α_{mn}), so that the co-polar and cross-polar far-field radiation components of the planar array, $FF_{cp}(\theta, \phi)$ and $FF_{xp}(\theta, \phi)$, satisfy the required specifications given in terms of upper and lower co-polar masks (UM and LM), and a cross-polar mask (CM), described by the limits imposed at P discrete angular directions (θ_p, ϕ_p). Thus, for the PSO algorithm, the vector C in (6) contains the parameters to be optimized and the fitness function to be minimized and used to weigh up the accuracy of any solution C, is given in (7). Basically, F in (7) consists of the errors associated with both $FF_{cp}(\theta, \phi)$ and $FF_{xp}(\theta, \phi)$ components, considering that far-fields along with the masks are normalized in amplitude and expressed in dB.

$$C = (a_{11}, \alpha_{11}, \ldots, a_{mn}, \alpha_{mn}, \ldots, a_{MN}, \alpha_{MN}) \qquad (6)$$

$$F = \sum_{p=1}^{P} \min(|FF_{cp}(dB)| - |UM(db)|, 0)$$

$$+ \sum_{p=1}^{P} \min(|LM(db)| - |FF_{cp}(dB)|, 0)$$

$$+ \sum_{p=1}^{P} \min(|FF_{xp}(dB)| - |CM(dB)|, 0) \qquad (7)$$

In PSO, for high-dimensional problems, the size of the swarm required may increase in such a way that the number of fitness evaluations rises up dramatically and thus, the computational cost. For large arrays, this problem can be reduced using an array consisting of subarrays. In this case, let us suppose a planar array consisting of $M \times N$ subarrays uniformly spaced d_x and d_y on the x and y axes, respectively; as shown in Fig. 1. Each subarray consists of $Q \times R$ microstrip patches uniformly spaced d_q and d_r on both directions. The array factor of the new arrangement is given by

$$AF(\theta, \phi) = \sum_{m=0}^{M-1} \sum_{n=0}^{N-1} a_{mn} \left(\sum_{q=0}^{Q-1} \sum_{r=0}^{R-1} b_{qr} \cdot e^{j(q \cdot k_x \cdot d_q + r \cdot k_y \cdot d_r + \beta_{qr})} \right)$$

$$\cdot e^{j(m \cdot k_x \cdot d_x + n \cdot k_y \cdot d_y + \alpha_{mn})} = AF(\theta, \phi)|_{M \times N} \cdot AF(\theta, \phi)|_{Q \times R} \qquad (8)$$

in which b_{qr} and β_{qr} represent the amplitude and phase of the excitation currents for each element within the subarray, and a_{mn} and α_{mn} represent complex excitation for each element within the array. Now, the vector C in (6) is modified in (9) by introducing the couples (b_{qr}, β_{qr}), identical for any of the subarrays, as well as the complex feeds for the $M \times N$ subarrays.

$$
\begin{aligned}
C = (&b_{11}, \beta_{11}, \ldots, b_{qr}, \beta_{qr}, \ldots, b_{QR}, \beta_{QR}, a_{11}, \alpha_{11}, \\
&\ldots, a_{mn}, \alpha_{mn}, \ldots, a_{MN}, \alpha_{MN})
\end{aligned} \tag{9}
$$

The use of subarrays makes it possible to reduce significantly the number of unknowns and the computational cost. For example, in case subarrays are not considered, a planar array consisting of $M \times N = 20 \times 20$ elements would require an 800-dimensions vector to be solved in (6) (400 couples (a_{mn}, α_{mn})), whereas if an array consisting of $M \times N = 10 \times 10$ subarrays is considered, with each subarray consisting of $Q \times R = 2 \times 2$ microstrip patches, then the vector C in (9) would be 208-dimensions in length (100 couples (a_{mn}, α_{mn}) for the array and 4 couples (b_{qr}, β_{qr}) for the subarray).

3. PARTICLE SWARM OPTIMIZATION

The PSO algorithm imitates in a computational fashion the coordinated and unpredictable movement of the particles within a swarm [1]. From a computational point of view, each particle's position corresponds to a potential solution to the optimization problem at hand in a D-dimensional search space, i.e., vectors C in (6) or (9).
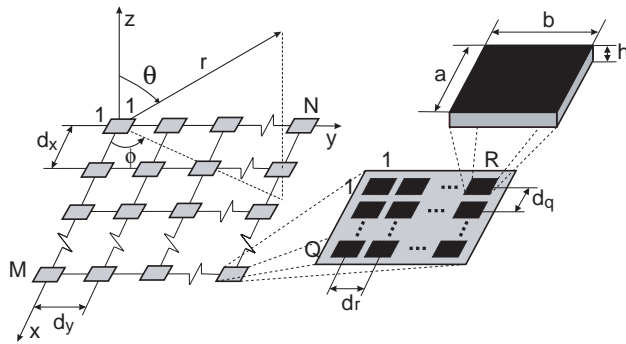

Figure 1. Planar array consisting of $M \times N$ subarrays uniformly spaced d_x and d_y on the x and y axes, respectively. Each subarray consists of $Q \times R$ microstrip patches uniformly spaced d_q and d_r on each direction.

The following subsections include a general overview of the classical real-valued PSO scheme considered [1, 22], along with a description of the elitist selection-based approach proposed.

3.1. Classical PSO

In PSO, a swarm consisting of K particles randomly initialized traverses the hyperspace iteratively towards more promising regions according to a velocity operator. Any particle k becomes a potential solution to the optimization problem at hand, and is represented by its current position in the D-dimensional search space, $X_k = (x_{k,1}, \ldots, x_{k,D})$. From iteration i to $i+1$, each particle moves from X_k^i to a new position X_k^{i+1} with a velocity $V_k^{i+1} = (v_{k,1}^{i+1}, \ldots, v_{k,D}^{i+1})$ as given by:

$$V_k^{i+1} = wV_k^i + c_1 r_1 \left(p_{best} - X_k^i \right) + c_2 r_2 \left(g_{best} - X_k^i \right) \qquad (10)$$

$$X_k^{i+1} = X_k^i + V_k^{i+1} \cdot \Delta t \qquad (11)$$

in which, w is the inertial weight, c_1 and c_2 are the cognitive and social acceleration constants, p_{best} and g_{best} represent the memory of the particle and the whole swarm, respectively; r_1 and r_2 are two independent random numbers, $U[0, 1]$, and Δt in (11) represents the time step between two consecutive movements [1, 3, 22].

The spatial movement and velocity of particles is iteratively delimited across any dimension d, by the intervals $x_d \in [x_{d,\min}, x_{d,\max}]$ and $v_d \in [-V_{\max}, V_{\max}]$, respectively. The limits $x_{d,\min}$ and $x_{d,\max}$ are related to the dynamic range of the variables to be optimized, and can be controlled by introducing a limiting wall, [3]. The maximum velocity allowed for particles on each dimension, $V_{\max}$, is usually set equal to or half the dynamic range, $V_{\max,d} = x_{d,\max} - x_{d,\min}$ or $V_{\max,d} = 0.5 \cdot (x_{d,\max} - x_{d,\min})$, respectively; and plays an important role in the final PSO performance [3, 22].

Several classical PSO schemes can be considered depending on how and when particles move and cooperate among themselves, i.e., depending on the application of the update rules given in (10)–(11). Among the classical PSO schemes, the one with asynchronous updates of the swarm and a global topology has been considered in this work as a reference, as it has proven to be the most efficient one in computational terms [18, 19, 22].

3.2. The Modified PSO

The modified PSO algorithm proposed introduces into the classical PSO flowchart [22] two mechanisms usually used in GA: a selection

operator, tournament selection (TS), and elitism [3]. In GA, TS increases the pressure over the search space, preserving iteratively one or more copies of the fittest individuals, which are the only ones that iteratively survive and take part in the reproduction cycle [2]. The greater the size of the subpopulation that competes in each tournament is, the higher the search pressure and convergence speed. However, subpopulations of $TS = 2$ individuals are often chosen, because if the subpopulation is too high, too many worse individuals can be lost, making diversity vanish and driving iteratively the algorithm to a deceptive local solution. In fact, TS itself promotes better solutions in such a way that high values of $V_{\max}$ must be chosen in PSO to overcome premature convergence.

The improvements achieved by introducing TS into the classical PSO have already been demonstrated by the authors in [19, 23]. Nevertheless, in this work elitism is also introduced. When TS is applied, it may happen that the best particle is not selected at random to compete in any tournament and lost. That means that the swarm may lose its global history, slowing down the search. Elitism forces the best particle to propagate iteratively even if the TS fails to choose it. The steps of the modified algorithm are summarized as follows:

i) Initialize the swarm: K particles with random positions and velocities, X_k and V_k. Evaluate their fitness, F_k, and set $p_{best,k}$ and g_{best}

ii) Until maximum number of iterations is reached
  ii.1) Repeat for all particles
    ii.1.1) Update velocity and position, V_k^{i+1} and X_k^{i+1}
    ii.1.3) Evaluate fitness, $F_k = f(X_k)$
    ii.1.4) Update personal best?, $p_{best,k} = X_k$
    ii.1.5) Update global best, g_{best}?
  ii.2) Next particle
  ii.3) TS: Apply K tournaments to build the new swarm
  ii.4) Elitism: Copy g_{best} to the new swarm if lost when applying TS

iii) Next iteration

iv) Solution: current g_{best}

v) END

4. RESULTS

Results comparing classical and modified PSO schemes along with representative synthesis results for sector antennas for WiMAX applications are presented in the following subsections.

4.1. Comparison of the PSO Schemes

The well-known Griewank, Rastrigin, Rosenbrock and Sphere test functions summarized in Table 1, with a zero-value global minimum [24], have been used as the test bed to compare the performance of both classical PSO with asynchronous updates of the swarm and a global topology (PSO hereinafter) and the same scheme modified by introducing TS and elitism (mPSO). For any of the functions and optimization algorithms, 100 independent runs have been considered to take into account the stochastic nature of the optimizers and carry out the analysis. The results obtained have been appropriately averaged to compare PSO and mPSO schemes, considering parameters such as the success rate (SR), representing the percentage of runs that converge to a valid solution, i.e., those runs for which the value of the function $f(x)$ reaches the specified value to reach (VTR), $f(x) < \text{VTR}$, with a maximum of 300000 fitness function calls allowed; and the average number of fitness function evaluations required to reach the VTR, NF_{avg}, computed considering only the successful runs. Finally, the following parameters have been considered for both PSO and mPSO algorithms based on previous experience [22]: $w = 0.729$, $c_1 = c_2 = 1.49445$, $V_{\max, d} = x_{d,\max} - x_{d,\min}$, reflecting wall [3], and a swarm with $K = 2D = 60$ particles.

Table 1. Test functions used to compare the PSO algorithms. For the D-dimensional functions, considering $D = 30$ dimensions, a parameter range and a value to reach, PR and VTR respectively, have been defined.

Function	Parameters
Griewank	$f(x) = 1 + \frac{1}{4000} \sum_{d=1}^{D} x_d^2 - \prod_{d=1}^{D} \cos\left(\frac{x_d}{\sqrt{d}}\right)$ PR: $x_d \in [-400, 400]$, VTR$= 0.1$
Rastrigin	$f(x) = \sum_{d=1}^{D} [x_d^2 - 10 \cdot \cos(2\pi x_d) + 10]$ PR: $x_d \in [-5.12, 5.12]$, VTR$= 90$
Rosenbrock	$f(x) = \sum_{d=1}^{D-1} [100 \cdot (x_{d+1} - x_d^2)^2 + (x_d - 1)^2]$ PR: $x_d \in [-2.048, 2.048]$, VTR$= 15$
Sphere	$f(x) = \sum_{d=1}^{D} x_d^2$ PR: $x_d \in [-100, 100]$, VTR$= 1 \cdot e^{-6}$

Table 2. Comparison of the PSO schemes. Results for the test functions considering 100 independent runs.

	PSO		mPSO	
	SR (%)	NF_{avg}	SR (%)	NF_{avg}
Griewank	100	14817.60	96	7895.10
Rastrigin	99	9152.73	88	4422.95
Rosenbrock	93	170272.90	100	36511.20
Sphere	100	27043.21	100	14889.10

For the test bed described in Table 1, results comparing PSO and mPSO are summarized in Table 2. According to the NF_{avg} parameter, which is directly related to the overall computational cost (approximately 99% of the CPU time is spent on fitness evaluations and the 1% remaining on basic PSO operations), it can be inferred from Table 2 that the mPSO scheme outperforms the PSO for any of the test functions considered, reducing the computational cost by up to 46.7%, 51.6%, 78.6% and 44.9% for the Griewank, Rastrigin, Rosenbrock and Sphere test functions, respectively. However, with regard to the SR parameter, both PSO and mPSO behave similarly, although for a high-complexity multimodal function such as Rastrigin, the mPSO failed in 12% of the runs, getting trapped in a local minimum in the surroundings of the global solution. This is the only limitation of the mPSO approach, as the pressure of TS and elitism together may drive the swarm to deceptive solutions with a slightly higher probability than the PSO.

Finally, let us suppose a canonical planar array synthesis problem to complete the comparison, considering: 1) a planar array with $M \times N = 8 \times 8$ microstrip patches and 2) a planar array consisting of $M \times N = 4 \times 4$ elements, in which each element is a subarray of $Q \times R = 2 \times 2$ microstrip patches. In the end, the number of radiating elements is the same in 1) and 2), but the feed network as well as the number of unknowns are quite different in both cases. Both problems can be formulated as a convex programming problem and solved more efficiently [25], but it also represents an appropriate example to compare both PSO and mPSO in a statistical way.

According to the geometry provided in Fig. 1, the dimensions of the antennas 1) and 2) are similar, given in terms of the free-space

wavelength, λ, as follows: 1) $d_x = 0.47\lambda$, $d_y = 0.55275\lambda$, $a = 0.25\lambda$, $b = 0.32275\lambda$, and 2) $d_x = 0.94\lambda$, $d_y = 1.1055\lambda$, $d_q = 0.47\lambda$, $d_r = 0.553\lambda$, $a = 0.25\lambda$, $b = 0.32275\lambda$; considering a CuClad 250 GX substrate with a permittivity of $\varepsilon_r = 2.4$ and a thickness of $h = 0.01167\lambda$. The far-field radiation pattern to fulfill is given in terms of 3D-masks defined in the intervals $\theta \in [-90, 90]$ and $\phi \in [0, 180]$ degrees. Fig. 2 shows a detail of the masks for a constant ϕ-cut. Moreover, the following parameters have been considered for both PSO and mPSO: $w = 0.729$, $c_1 = c_2 = 1.49445$, $V_{\max, d} = 0.5 \cdot (x_{d, \max} - x_{d, \min})$, reflecting wall and a size of the swarm of $K = D/2$, i.e., 64 and 20 particles for 1) and 2), respectively, as vector C in (6) and (9) is 128 and 40-dimensions in length, respectively.

Furthermore, the dynamic range in vector C for the complex weights to be optimized, are for both configurations: 1) $a_{mn} \in [0, 1]$ and $\alpha_{mn} \in [0, 360]$, and 2) $b_{qr} \in [0, 1]$ and $\beta_{qr} \in [0, 360]$. Then, for both antennas 1) and 2), the aim is to optimize the 128 and 40-dimensions vector C, respectively; in order to satisfy the requirements of the 3D-masks proposed, minimizing the residual error given in (7).

As an example, Fig. 2 shows for both kinds of planar arrays the far-field results for the 0 degrees ϕ-cut, obtained with the mPSO algorithm for a single run, showing a good agreement in both cases.

In order to complete the analysis, statistical results comparing both PSO and mPSO schemes for the planar arrays described in 1) and 2), are shown in Table 3. In this case, the results of 25 independent
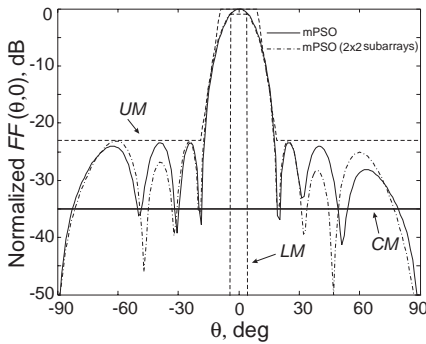
Figure 2. Representative synthesis results for the 0 degrees ϕ-cut, considering a $M \times N = 8 \times 8$-elements planar array ($M \times N = 4 \times 4$ in case a $Q \times R = 2 \times 2$ subarray is considered).
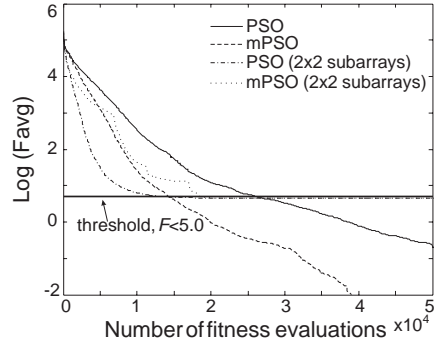
Figure 3. Evolution of the averaged fitness value for the $M \times N = 8 \times 8$-elements planar array ($M \times N = 4 \times 4$ in case a $Q \times R = 2 \times 2$ subarray is considered).

Table 3. Comparison of the PSO schemes. Results for a planar array when averaging 25 independent runs.

	PSO		mPSO	
	SR (%)	*NF*$_{avg}$	*SR* (%)	*NF*$_{avg}$
No subarrays *M×N=8×8*	100	22917.12	100	12910.08
Array with subarrays *M×N=4×4* and *Q×R=2×2*	100	10219.20	96	11707.50

runs have been properly averaged, considering that a run converges to a valid solution only if $F < 5.0$ in (7), with a maximum of 50000 fitness function calls allowed. Results in Table 3, as well as the evolution of the averaged fitness value shown in Fig. 3 and drawn considering only successful runs, demonstrate for case 1) (antenna with no subarrays), the computational superiority of the mPSO over the PSO. In fact, the reduction in the NF_{avg} parameter is significant, close to a 44%. However, for case 2) (antenna with subarrays), the mPSO behaves slightly worse than the PSO. The reason is that in this case the mPSO works with such a small population ($K = 20$ particles) that the TS and elitism altogether reduce the exploration abilities of the swarm, making the search more difficult; i.e., from the beginning the swarm is driven by one or more copies of the same particles, reducing diversity and slowing down the convergence.

Finally, if the evolutions of PSO and mPSO shown in Fig. 3 for cases 1) and 2) are compared, it can be concluded that the antenna with subarrays, case 2), exhibits a far slower convergence with both algorithms. Obviously, the requirements of the masks are the same, but in case 2) there are very few excitations or variables to fit the far-field diagram of the planar array and besides, the size of the swarm for the PSO-based schemes is far smaller, reducing the exploration abilities of the algorithms.

4.2. Sector Antennas for WiMAX

Focusing on the mPSO scheme, the optimization algorithm has also been applied to more realistic and complex synthesis problems. Let us consider a planar array to be used as a 60 degrees sector antenna for WiMAX applications at 3.5 GHz, providing horizontal polarization. The required beam is shaped both in azimuth and elevation, and the 3D radiation pattern is specified as the product of sectored and cosecant squared patterns [26]. Even though problems defined by separable

masks can be solved more efficiently using other methods like the one described in [27] (which does not consider crosspolar masks), this problem has got enough complexity to check the performance of the global optimization algorithm proposed.

Regarding the planar array, two possibilities are considered again according to the geometry shown in Fig. 4(a): 1) a planar array with $M \times N = 16 \times 16$ microstrip patches and 2) a planar array consisting of $M \times N = 8 \times 8$ subarrays of $Q \times R = 2 \times 2$ microstrip patches each. Moreover, the dimensions in cm of the antennas 1) and 2), are as follows: 1) $d_x = 3.428571$, $d_y = 4.052131$, $a = 2.142857$, $b = 2.766417$, and 2) $d_x = 6.857143$, $d_y = 8.104262$, $d_q = 3.428571$, $d_r = 4.052131$, $a = 2.142857$, $b = 2.766417$; considering again the CuClad 250 GX substrate with $\varepsilon_r = 2.4$ and $h = 1\,\text{mm}$.
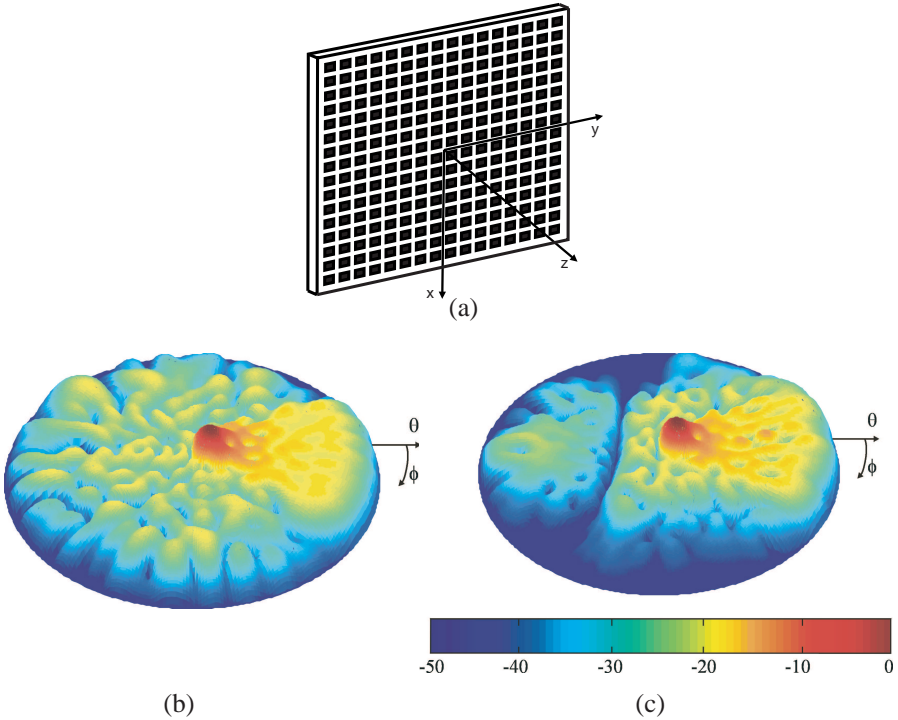

Figure 4. 3D far-field radiation pattern obtained for a 60-degrees sector antenna. (a) Geometry of the planar array. (b) Results for a planar array consisting of $M \times N = 16 \times 16$ microstrip patches. (c) Results for a planar array consisting of $M \times N = 8 \times 8$ subarrays with $Q \times R = 2 \times 2$ microstrip patches each one.

The following parameters have been considered for the mPSO: $w = 0.729$, $c_1 = c_2 = 1.49445$, $V_{\max, d} = 0.5 \cdot (x_{d, \max} - x_{d, \min})$, reflecting wall and a size of the swarm of $K = D/2$, i.e., 256 and 68 particles for 1) and 2), respectively. Furthermore, the dynamic ranges in vector C for the complex weights to be optimized, are for both configurations: 1) $a_{mn} \in [0, 1]$ and $\alpha_{mn} \in [0, 360]$, and 2) $b_{qr} \in [0, 1]$ and $\beta_{qr} \in [0, 360]$.

Representative results achieved for a single run showing the 3D-normalized far-field radiation pattern synthesized with the mPSO for both sector antennas 1) and 2), are presented in Figs. 4(b)–(c). From the normalized polar representation shown in Figs. 4(b)–(c), the cosecant squared behavior within the angular limits of the sector can be inferred. Further details of these accurate results are shown in Fig. 5, including the elevation and azimuth cuts for both sector antennas, demonstrating the usefulness of the mPSO approach. From a practical point of view, the nature of the synthesis would make it necessary to use electronically controlled amplifiers and phase shifters to implement the optimized complex feeds.
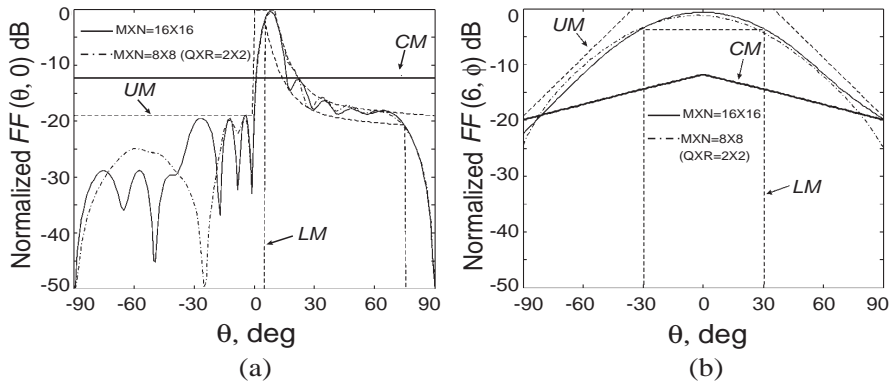

Figure 5. Elevation and azimuth cuts of the far-field radiation pattern for the 60 degrees sector antennas. The cross-polar component is below the $-50\,\mathrm{dB}$ floor level considered. (a) Elevation cut, $\phi = 0$ degrees. (b) Azimuth cut, $\theta = 6$ degrees.

5. CONCLUSION

A modified particle swarm based optimization algorithm that combines the capacity of the heuristic PSO technique to find a near-optimal solution in a multimodal and high-dimensional search domain, with the skill of genetic operators such as tournament selection and elitism

to speed up the search by filtering iteratively the population and promoting the survival of the fittest individuals, has been presented in this work and compared to classical PSO, using several well-known test functions as benchmark functions, as well as a canonical planar array synthesis task using complex weights.

The statistical results obtained with the test functions for both PSO schemes demonstrate that the modified PSO is computationally more efficient than the classical one, outperforming it. The only drawback associated with the approach proposed is related to the pressure exerted by selection and elitism altogether, which may lead in some cases to a premature convergence due to the lack of diversity inside the swarm. Similar conclusions have been obtained when both optimization schemes have been applied to planar array synthesis. In this case, two different antenna structures have been used, considering either microstrip patches or subarrays of microstrip patches as the elements of the planar array. Both architectures have been tested, and the one using subarrays has proven to be the most efficient one from the optimizer point of view, as it reduces the unknowns or excitation currents significantly. However, for antennas with few elements and in case subarrays are considered, results have demonstrated that the residual error is higher, i.e., the convergence is slower, because the small size of the swarm makes the exploration of the search space more difficult.

Finally, the high-accurate synthesis results of a sector antenna for WiMAX applications, demonstrate the usefulness of the approach proposed for more realistic electromagnetic problems.

REFERENCES

1. Kennedy, J. and R. C. Eberhart, *Swarm Intelligence*, Morgan Kaufmann, San Francisco, 2001.

2. Rahmat-Samii, Y. and E. Michielssen, *Electromagnetic Optimization by Genetic Algorithms*, John Wiley & Sons, New York, 1999.

3. Robinson, J. and Y. Rahmat-Samii, "Particle swarm optimization in electromagnetics," *IEEE Trans. Antennas Propagat.*, Vol. 52, No. 2, 397–407, 2004.

4. Coleman, C. M., E. J. Rothwell, and J. E. Ross, "Investigation of simulated annealing, ant-colony optimization, and genetic algorithms for self-structuring antennas," *IEEE Trans. Antennas Propagat.*, Vol. 52, No. 4, 1007–1014, 2004.

5. Lim, T. S., V. C. Koo, H. T. Ewe, and H. T. Chuah, "A

sar autofocus algorithm based on particle swarm optimization," *Progress In Electromagnetics Research B*, Vol. 1, 159–176, 2008.

6. Lee, K. C., C. W. Huang, and Y. H. Chen, "Analysis of nonlinear microwave circuits by particle swarm algorithm," *Journal of Electromagnetic Waves and Applications*, Vol. 21, No. 10, 1353–1365, 2007.

7. Li, J. F., B. H. Sun, Q. Z. Liu, and L. Gong, "PSO-based fast optimization algorithm for broadband array antenna by using the cubic spline interpolation," *Progress In Electromagnetics Research Letters*, Vol. 4, 173–181, 2008.

8. Mahmoud, K. R., M. El-Adawy, S. M. M. Ibrahem, R. Bansal, and S. H. Zainud-Deen, "Performance of circular Yagi–Uda arrays for beamforming applications using particle swarm optimization algorithm," *Journal of Electromagnetic Waves and Applications*, Vol. 22, No. 2–3, 353–364, 2008.

9. Zainud-Deen, S. H., W. M. Hassen, E. El deen Ali, and K. H. Awadalla, "Breast cancer detection using a hybrid finite difference frequency domain and particle swarm optimization techniques," *Progress In Electromagnetics Research B*, Vol. 3, 35–46, 2008.

10. Chen, T. B., Y. L. Dong, Y. C. Jiao, and F. S. Zhang, "Synthesis of circular antenna array using crossed particle swarm optimization algorithm," *Journal of Electromagnetic Waves and Applications*, Vol. 20, No. 13, 1785–1795, 2006.

11. Li, W. T., X. W. Shi, and Y. Q. Hei, "An improved particle swarm optimization algorithm for pattern synthesis of phased arrays," *Progress In Electromagnetics Research*, PIER 82, 319–332, 2008.

12. Liu, X. F., Y. B. Chen, Y. C. Jiao, and F. S. Zhang, "Modified particle swarm optimization for patch antenna design based on IE3D," *Journal of Electromagnetic Waves and Applications*, Vol. 21, No. 13, 1819–1828, 2007.

13. Chamaani, S., S. A. Mirtaheri, M. Teshnehlab, M. A. Shoorehdeli, and V. Seydi, "Modified multi-objective particle swarm optimization for electromagnetic absorber design," *Progress In Electromagnetics Research*, PIER 79, 353–366, 2008.

14. Li, W.-T., X.-W. Shi, L. Xu, and Y.-Q. Hei, "Improved ga and pso culled hybrid algorithm for antenna array pattern synthesis," *Progress In Electromagnetics Research*, PIER 80, 461–476, 2008.

15. Grimaccia, F., M. Mussetta, and R. E. Zich, "Genetical swarm optimization: Self-adaptive hybrid evolutionary algorithm for electromagnetics," *IEEE Trans. Antennas Propagat.*, Vol. 55, No. 3, 781–785, 2007.

16. Boeringer, D. W. and D. H. Werner, "Particle swarm optimization versus genetic algorithms for phased array synthesis," *IEEE Trans. Antennas Propagat.*, Vol. 52, No. 3, 771–779, 2004.

17. Jin, N. and Y. Rahmat-Samii, "Advances in particle swarm optimization for antenna designs: Real-number, binary, singleobjective and multiobjective implementation," *IEEE Trans. Antennas Propagat.*, Vol. 55, No. 3, 556–567, 2007.

18. Perez, J. R. and J. Basterrechea, "Particle swarms applied to array synthesis and planar near-field antenna measurement," *Microwave Opt. Technol. Lett.*, Vol. 50, No. 2, 544–548, 2008.

19. Perez, J. R. and J. Basterrechea, "Particle swarm optimization with tournament selection for linear array synthesis," *Microwave Opt. Technol. Lett.*, Vol. 50, No. 3, 627–632, 2008.

20. Balanis, C. A., *Antenna Theory*, John Wiley & Sons, New Jersey, 2005.

21. Ludwig, A. C., "The definition of cross polarization," *IEEE Trans. Antennas Propagat.*, Vol. 21, No. 1, 116–119, 1973.

22. Perez, J. R. and J. Basterrechea, " Particle-swarm optimization and its application to antenna far-field-pattern prediction from planar scanning," *Microwave Opt. Technol. Lett.*, Vol. 44, No. 5, 398–403, 2005.

23. Pérez, J. R. and J. Basterrechea, "Hybrid particle swarm–based algorithms and their application to linear array synthesis," *Progress In Electromagnetics Research*, PIER 90, 63–74, 2009.

24. Clerc, M. and J. Kennedy, "The particle swarm-explosion, stability, and convergence in a multidimensional complex space," *IEEE Trans. Evolutionary Comp.*, Vol. 6, No. 1, 58–73, 2002.

25. Isernia, T., P. D. Iorio, and F. Soldovieri, "An effective approach for the optimal focusing of array fields subject to upper bounds," *IEEE Trans. Antennas Propagat.*, Vol. 48, No. 12, 1837–1847, 2000.

26. ETSI EN 302 085 v1.2.3, "Fixed radio systems; point-to-multipoint antennas; antennas for point-to-multipoint fixed radio systems in the 3 GHz to 11 GHz band," *European Standard (Telecommunications Series)*, 2005.

27. Isernia, T., O. M. Bucci, and N. Fiorentino, "Shaped beam antenna synthesis problems: Feasibility criteria and new strategies," *Journal of Electromagnetic Waves and Applications*, Vol. 12, No. 1, 103–138, 1998.